Accepted Article

This manuscript has been accepted after peer review and appears as an Accepted Article online prior to editing, proofing, and formal publication of the final Version of Record (VoR). This work is currently citable by using the Digital Object Identifier (DOI) given below. The VoR will be published online in Early View as soon as possible and may be different to this Accepted Article as a result of editing. Readers should obtain the VoR from the journal website shown below when it is published to ensure accuracy of information. The authors are responsible for the content of this Accepted Article.

Highly Stable Aqueous Zinc-ion Storage Using Layered Calcium Vanadium Oxide Bronze Cathode

Chuan Xia, Jing Guo, Peng Li, Xixiang Zhang and Husam N. Alshareef*

Abstract: Cost-effective aqueous rechargeable batteries are attractive alternatives to non-aqueous cells for stationary grid energy storage. Among different aqueous cells, zinc-ion batteries (ZIBs), based on Zn^{2+} intercalation chemistry, stand out as they can employ high-capacity Zn metal as anode material. Herein, we report a layered calcium vanadium oxide bronze as cathode material for aqueous Zn batteries. For the storage of Zn^{2+} ions in aqueous electrolyte, we demonstrate that calcium based bronze structure can deliver a high capacity of 340 mAh g^{-1} at 0.2 C, good rate capability and very long cycling life (96% retention after 3000 cycles at 80 C). Further, we investigate the Zn^{2+} storage mechanism, and the corresponding electrochemical kinetics in this bronze cathode. Finally, we show that our Zn cell delivers an energy density of 267 Wh kg^{-1} at a power density of 53.4 W kg^{-1}.

Aqueous rechargeable batteries are a promising class of batteries for grid-scale electrochemical energy storage.[1] This is largely because of their low-cost and operational safety. Further, it is well known that aqueous electrolytes offer much higher ionic conductivities (∼1 S cm^{-1}), compared to non-aqueous electrolytes (∼1-10 mS cm^{-1}), which favors high-rate capabilities.[2]. Efforts in large-scale aqueous energy storage has spanned naturally abundant Na^+ and K^+ intercalation materials,[3] as well as multivalent charge carriers (e.g., Zn^{2+}, Ca^{2+}, Mg^{2+}, and Al^{3+}).[4] Obviously, rechargeable cells employing multivalent ions can, in principle, deliver higher storage capacity due to multiple electron transfers. Among them, aqueous zinc-ion batteries (ZIBs), based on Zn^{2+} intercalation chemistry, stand out owing to the following properties of Zn anode: 1) high capacity (820 mAh g^{-1}; 5851 mAh mL^{-1}); 2) high-abundance, and low-cost;[1b] 3) low redox potential (−0.76 V vs. standard hydrogen electrode);[5] and 4) impressive electrochemical stability in water due to a high overpotential for hydrogen evolution.[2] Moreover, replacement of the alkaline electrolyte by mild neutral pH (or slightly acidic) solution can virtually eliminate the dendritic zinc issues, which prevail in alkaline zinc cells; and simultaneously decrease the environmental impact and maintenance cost.[6] One of the main challenges which hinder the practical application of aqueous ZIBs is the lack of suitable intercalation cathodes, which can offer high capacity and good structure stability during Zn^{2+} (de)intercalation.

Thus, the development of high performance ZIB cathode is a prerequisite to achieve stable aqueous zinc-ion storage.

In the early stages of development, polymorphous of MnO_2 were seriously investigated as potential Zn^{2+} host materials.[1a, 7] Afterwards, Prussian blue analogs were proposed to realize stable aqueous ZIBs.[8] Unfortunately, these electrodes suffer from either limited capacity or very poor cycling stability. Very recently, layered and hydrated V_2O_5 derivatives (e.g. $Zn_{0.25}V_2O_5$ nH_2O)[2] were reported as high-performance ZIB cathodes, which delivered high capacity (>300 mAh g^{-1}) and long-term cycling stability (>1000 cycles), as well as impressive rate capability. Such performance improvements were mainly attributed to the following reasons: 1) their open-framework crystal structure which has pillars between V_2O_5 bilayers (leading to expanded interlayer spacing), which insures fast and reversible Zn^{2+} insertion/removal. In addition, compared with monovalent alkali metal cations (e.g. Li^+, Na^+, K^+), the divalent metal ions bonded with oxygen atoms can bring about stronger ionic bonds,[9] better binding of the layers together, which effectively prevents structural collapse; 2) the tendency of vanadium to exist in multiple oxidation states, hence making it high-capacity in principle; 3) the charge shield effect of the crystal H_2O, which could reduce the effective charges of intercalated Zn^{2+} ions, and thus enhance the capacity and rate performance.[6, 10] To capitalize on these features, herein, we propose double-layered calcium vanadium oxide bronze ($Ca_{0.25}V_2O_5$ nH_2O or CVO) as more suitable aqueous ZIB intercalation cathode compared to $Zn_{0.25}V_2O_5$ nH_2O for the following considerations: 1) compared to ZnO_6 octahedra pillars in $Zn_{0.25}V_2O_5$ nH_2O compound, the larger CaO_7 polyhedra in CVO may further expand the cavity size between V_4O_{10} layers; 2) the smaller molecular weight and density of CVO probably can give higher gravimetric and volumetric capacity; 3) the CVO offer 4-folds higher electrical conductivity than $Zn_{0.25}V_2O_5$ nH_2O, as demonstrated later. We show that freestanding CVO paper cathode deliver capacities of 340 and 289 mAh g^{-1} at 0.2 and 1 C, respectively. The fast electrochemical kinetics of CVO is also quantitatively illustrated using cyclic voltammetry. We demonstrate that, even when cycled at 80 C, the CVO cathode retain ∼96% and ∼78% of its initial capacity after 3000 and 5000 cycles, respectively. A highly reversible Zn^{2+} intercalation mechanism is elucidated using *ex-situ* X-ray diffraction (XRD), X-ray photoelectron spectroscopy (XPS) and transmission electron microscope (TEM) studies.

The CVO sample was synthesized using a one-step hydrothermal method (see supporting information for details). As shown in **Fig. 1a** and supporting **Fig. S1**, the crystal structure of CVO is very similar as δ-type $Zn_{0.25}V_2O_5$ nH_2O.[11] Both of these oxides can be described in a common manner where V_2O_5 layers stack along

[*]   C. Xia, J. Guo, Dr. P. Li, Prof. X.X. Zhang, Prof. H.N. Alshareef
       Materials Science and Engineering
       King Abdullah University of Science and Technology (KAUST)
       Thuwal 23955-6900, Saudi Arabia
       E-mail: husam.alshareef@kaust.edu.sa

[ ]   These authors contributed equally to this work

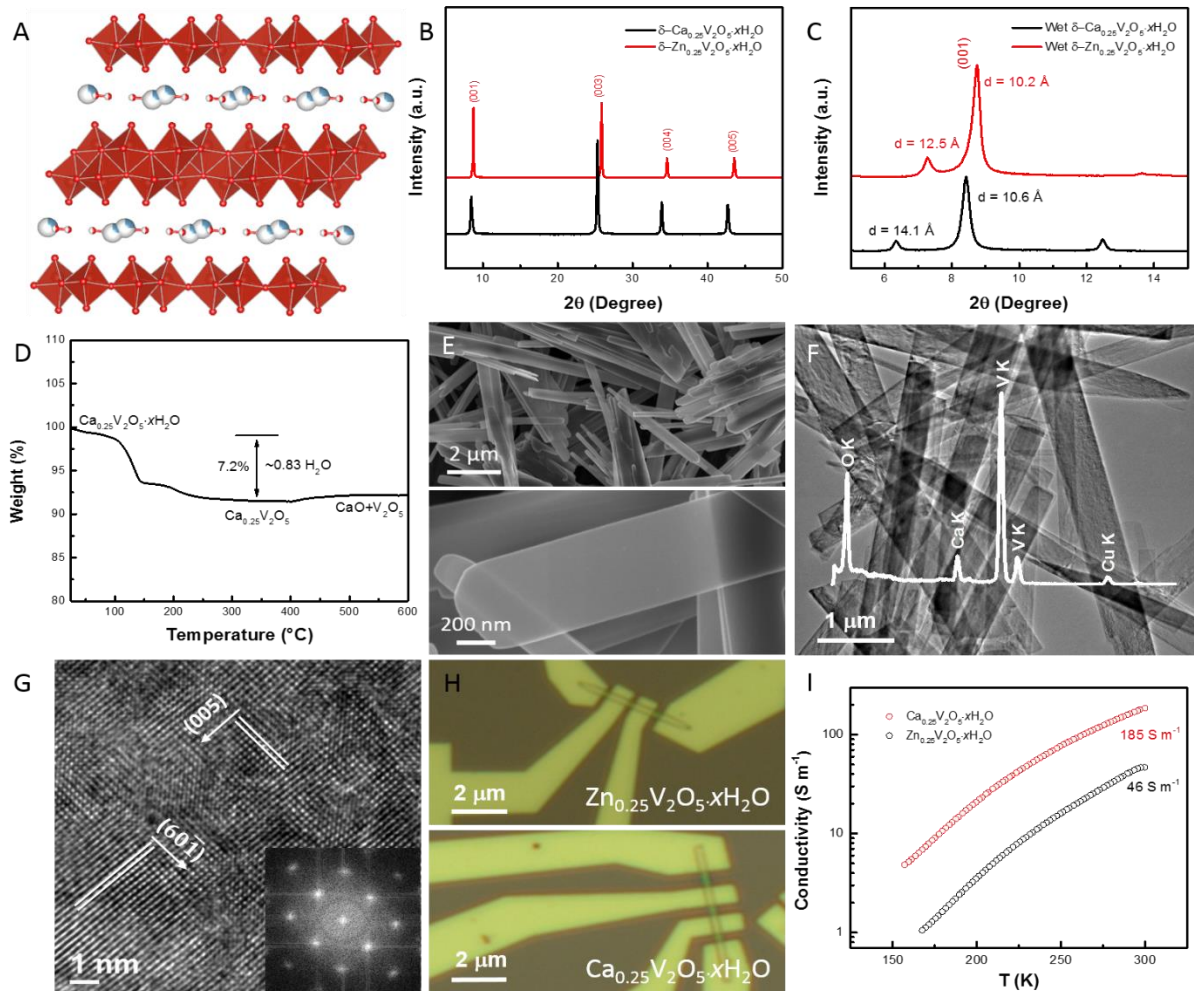   Supporting information for this article is given via a link at the end of the document.

Fig.1. A) Crystal structure viewed along the b-axis of CVO, which shows a double-layered structure with open-framework. The V atoms in V_2O_5 polyhedra are depicted in red. The blue-white and red-white atoms in the crystal represent the intercalated Ca ions and lattice water, respectively. B-C) Typical XRD pattern of as-synthesized CVO. D) TGA results on CVO samples. E-G) SEM and TEM images of CVO nanobelts. Inset in (F) shows the EDS spectrum of as-obtained CVO, showing the existence of O, Ca, and V elements. The Ca/V atomic ratio is *ca.* 0.13. H) The individual CVO and $Zn_{0.25}V_2O_5$ nH_2O based nanodevices, and I) their corresponding electricity conductivities.

the *c* axis and the intercalated metal ions (Zn^{2+} or Ca^{2+}) as well as water molecules reside in the interlayer space.[12] The intercalated metal ions can strongly bond to V_2O_5 layers and H_2O to form polyhedra pillars (ZnO_6 and CaO_7), which expand the interlayer gap of V_2O_5 and make the formed crystal more stable. However, the Ca-O bonds in CaO_7 pillars (2.38~2.57 Å)[12] are much longer than Zn-O bonds (2.03~2.13 Å)[11] in $Zn_{0.25}V_2O_5$ nH_2O, implying that an increased interlayer space is expected for the CVO crystal. The XRD analysis supports our hypothesis. As displayed in **Fig. 1b**, the XRD pattern of pristine CVO is dominated by (00*l*) reflections, revealing a high degree of preferred orientation along the *c* axis. Further, the absence of any impurity peaks demonstrates the single-phase nature of as-prepared CVO. The downshift of the diffraction angle corresponding to (00*l*) peaks of CVO compared to $Zn_{0.25}V_2O_5$ nH_2O confirms its larger interlayer distance along (00*l*) direction. We also found that the V_2O_5 open-framework of CVO allows the insertion of water molecules from the electrolyte into its interlayer space, in agreement with previous report.[2] The XRD result (**Fig.1c**) indicates that the interlayer space of CVO increased from 10.6 to 14.1 Å upon immersion in electrolyte, corresponding to water intercalation. Of note, the

pristine XRD pattern can be recovered by vacuum drying. Apparently, more water molecules can be intercalated into CVO lattice (3.5 Å increase of interlayer space) compared to $Zn_{0.25}V_2O_5$ nH_2O (2.3 Å increase of interlayer space), confirming a more open crystal structure for CVO. This feature may facilitate the electrochemical (de)intercalation of Zn^{2+} ions into CVO crystal. Inductively coupled plasma optical emission spectroscopy (ICP-OES) and thermogravimetric (TGA) studies (**Fig.1d**) further reveal that the stoichiometric formula for the as-prepared calcium vanadium oxide bronze is $Ca_{0.24}V_2O_5$ $0.83H_2O$.

Scanning electron microscope (SEM) images reveal a typical nanobelt morphology with smooth surface of as-synthesized CVO (**Fig. 1e**), which show the nanobelts to be a few micrometers long and several hundred nanometers wide. The representative TEM images (**Fig. 1f-g**) further illustrate the flat ribbon morphology and single-crystallinity of CVO materials. A lattice fringe with d-spacing of 0.196 and 0.211 nm can be observed in the high-resolution TEM image, corresponding to (‾) and (005) planes of CVO nanobelt, respectively. The elemental composition of the nanobelt was investigated by energy-dispersive X-ray

spectroscopy (EDS) (inset in **Fig.1f**) and the result shows that the atomic ratio of Ca to V is *ca.* 0.13, which is close to that of $Ca_{0.24}V_2O_5$ $0.83H_2O$. Additionally, we show that the CVO nanobelts are typically 50~60 nm thick, as determined by atomic force microscopy (supporting **Fig. S2**). Considering the importance of electrical conductivity of electrode materials for energy storage applications, we then precisely measured the electrical conductivities of as-prepared samples using individual nanobelt based nanodevices (**Fig. 1h**). As shown in **Fig. 1i**, the CVO sample offers a 4-fold higher electrical conductivity than previously reported $Zn_{0.25}V_2O_5$ nH_2O nanobelt at room-temperature. Undoubtedly, the higher electrical conductivity can boost the electron transfer during Zn^{2+} (de)intercalation, thereby enhancing battery performance.

The freestanding CVO paper electrode was used as cathode in aqueous ZIB, where the zinc metal and 1.0 M $ZnSO_4$ aqueous solution were used as anode and electrolyte, respectively. The CVO paper electrode ([1] 5.7 mg cm^{-2}) was prepared using a vacuum filtration method (see experimental section). The Zn//CVO cells were cycled in a voltage window of 0.6~1,6 V versus Zn, considering the structural stability of cathode materials. As shown in supporting **Fig. S3a**, in such a voltage window the Zn cell is very robust. Supporting **Fig. S3b** shows the 1st, 2nd, 5th and 10th cycle of the cyclic voltammetry (CV) curves at a scan rate of 0.1 mV s^{-1}. Multiple pairs of redox peaks are observed, demonstrating a multistep reaction mechanism associated with Zn^{2+} insertion/extraction. The CV study implies that the Zn^{2+} (de)intercalation process in Zn//CVO cell is highly reversible since no obvious peak current losses are observed from 2nd to 10th CV scans. **Fig. 2a** shows the galvanostatic charge-discharge (CD) profiles at various current densities. A high initial capacity of 340 mAh g^{-1} is achieved at 0.2 C. The predominantly sloping CD curves suggest fast kinetics which originate from the solid-solution type process. To further understand the electrochemical kinetics of CVO cathode, we quantified the capacitive and diffusion limited contributions to the total capacity using previously reported approach by Dunn and co-workers.[13] **Fig. 2b** exhibits the CV curves of CVO electrode from 0.2 to 0.5 mV s^{-1}. With increasing scan rates, the CV curves maintain the same shape with subtle shifting of redox peaks. The results, summarized in **Fig. 2c**, show that at a scan rate of 0.3 mV s^{-1}, 76% of the current can be attributed to the capacitive response of the CVO cathode, clearly revealing that the corresponding solid-solution reactions are mainly limited by the electrochemical reaction rate themselves instead of the mobile ion diffusion rate. Further, we employed the galvanostatic intermittent titration technique (GITT) to estimate the Zn^{2+} ion diffusion coefficient in CVO cathode (see details in supporting **Fig. S4**). Despite the divalent nature of the Zn^{2+} ion, the GITT-determined diffusion coefficient is still as high as [1] $F\in$ [8] to 10^{-9} cm^2 s^{-1}. The above discussion clearly demonstrates the fast kinetics of as-prepared CVO materials, and imply their good rate capability.

The rate performance of our CVO cathode is illustrated in **Fig. 2d**, where the current density was increased step-wise from 0.2 to 80 C and returned to 0.2 C. It is obvious that the CVO electrodes retain 85% of the initial specific capacity when current increases from 0.2 (340 mAh g^{-1}) to 1 C (289 mAh g^{-1}), outperforming

previously reported $Zn_{0.25}V_2O_5$ nH_2O (300 and 282 mAh g^{-1} at 1/6 and 1 C, respectively). Even at a fast charge-discharge rate of 80 C (45 s), these CVO electrodes still offer a high capacity of 72 mAh g^{-1} due to the fast Zn^{2+} ion migration. Of note, the capacity of these CVO electrodes recovered to 323 mAh g^{-1} (95%) when the current density was returned to 0.2 C, suggesting excellent structural stability. We also note that the CVO cathodes do not show notable capacity decay over at least 3000 cycles ([1] 96% retention) even at very high current density of 80 C (**Fig. 2e**). In contrast, the $Zn_{0.25}V_2O_5$ nH_2O cathode show 19% capacity decay only after 1000 cycles at 8 C rate.[2] It is worthwhile to note that Columbic efficiency of CVO cathode during cycling tests is close to 100%, confirming that the impressive cycling performance is not due to parasitic reactions. **Figure 2f** shows the Ragone plot of our Zn//CVO cell, in comparison to other reported intercalation Zn cells. Impressively, our devices show a very high energy density of 267 Wh kg^{-1} at a power density of 53.4 W kg^{-1}. Even when charging the cell within 45 s, the energy density is still as high as 133 Wh kg^{-1} at an outstanding power density of 1825 W kg^{-1}. Furthermore, it can be seen that our cells offer better performance than cells based on $Zn_3V_2O_7(OH)_2$,[14]
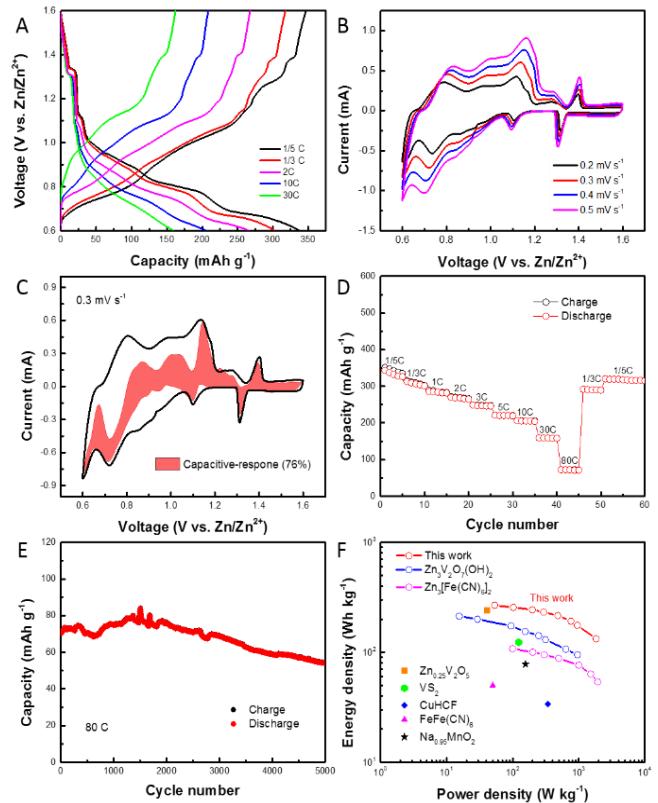

Fig.2. A) Galvanostatic charge. discharge profiles for CVO electrodes at different current densities. B) Cyclic voltammetry curves of CVO electrodes at various scan rates. C) Capacity separation analysis at 0.3 mV s^{-1}. The red-shaded data show the contribution to capacitive charge storage as a function of potential. D) Rate performance of CVO cathodes. E) Cycle performance at a current rate of 80 C. F) The Ragone plot of Zn//CVO cell in comparison with other aqueous ZIBs.

$Zn_{0.25}V_2O_5$ nH_2O,[2] $Zn_3[Fe(CN)_6]_2$[8a] CuHCF,[8b] VS_2,[15] $FeFe(CN)_6$,[16] and $Na_{0.95}MnO_2$[17] cathodes.

The successful and stable aqueous storage of Zn^{2+} in CVO cathode can be demonstrated by *ex-situ* high-resolution XPS

analysis. As shown in **Fig. 3a**, there is no Zn signal in the initial state for CVO cathode. However, the Zn 2p peaks ($2p_{3/2}$: 1022 eV)[18] emerge when the CVO electrodes were discharged to 0.6 V. The newly evolved Zn peaks clearly demonstrate the successful insertion of Zn^{2+} ions into porous CVO lattice. Next, we show that the CaO_7 pillars are quite stable during Zn^{2+} incorporation. Specifically, we do not observe any intensity decrease for Ca 2p peaks as we go from initial state to fully discharged state (**Fig. 3b-c**). Further, it is worthwhile to note that

interlayer spacing of layered intercalation cathode should be expanded after guest ion incorporation. However, a small contraction (*ca.* 5.7%) of the CVO lattice (10.6 Å for (001) planes) is observed when discharged to 0.6 V (10 Å for (001) planes). This is likely due to increased screening of the interlayer electrostatic repulsion as the Zn^{2+} insertion and the expulsion of water molecules from the interlayer, which has been demonstrated by Nazar and co-workers.[2] Moreover, even after continuous 100 CD cycles, the CVO cathode can perfectly preserve its crystal
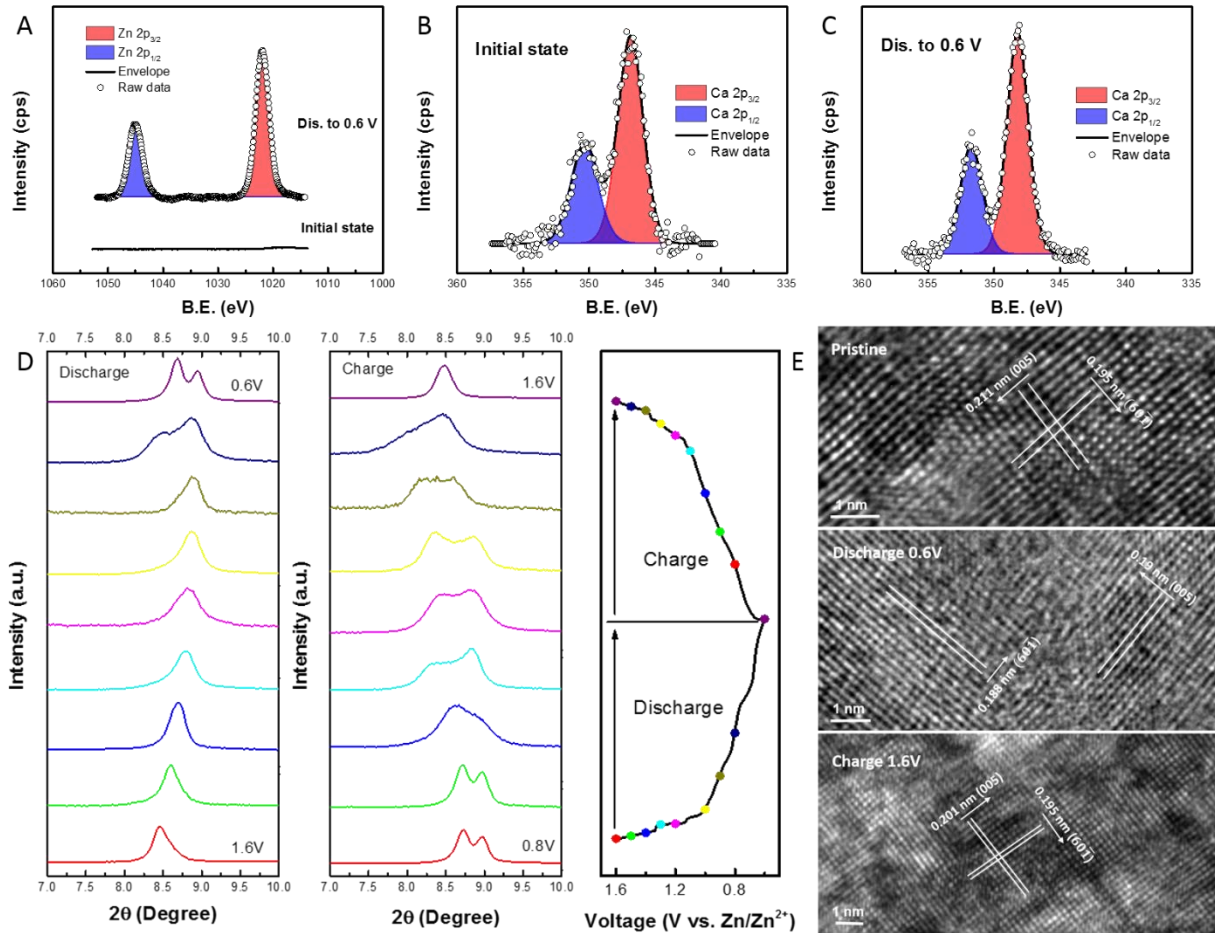

Fig.3. *Ex-situ* high-resolution XPS spectra of the A) Zn 2p and B-C) Ca 2p regions in pristine and fully discharged state of the CVO electrodes. D) *Ex-situ* XRD patterns of (001) Bragg peak of the CVO cathode 3rd charge–discharge scan as a function of discharge and charge voltage. E) *Ex-situ* high-resolution TEM images of the CVO nanobelt at initial, fully discharged (0.6 V) and charged state (1.6 V).

fully discharged CVO electrode shows only one Ca 2p component (Ca^{2+}), implying that the CaO_7 pillars are not partially reduced as a consequence of $Zn^{2+}/2e^-$ intercalation. The blue shift (346.9 eV for pristine CVO; 348.1 eV for discharged state) of binding energy for Ca^{2+} component in fully discharged CVO cathode is linked to the intercalation of the Zn^{2+} ions. A very similar blue shift was previously observed in Cr intercalated $CaCO_3$ system.[19] In order to gain better insight into the electrochemical process during Zn^{2+} (de)intercalation, *ex-situ* XRD analysis was carried out. Supporting **Fig. S5** shows that (00*l*) Bragg peaks corresponding to CVO phase shift to higher angles in the fully discharged state (0.6 V), and nearly return to their initial positions upon discharging to 1.6 V. Obviously, the CVO cathode does not undergo a phase evolution following Zn^{2+} insertion and extraction. Typically, the

structure without impurities formation, e.g. basic zinc sulfate. The 100 times cycled CVO electrode retained a 10.3 Å interlayer spacing, similar to the 10.6 Å interlayer spacing observed in fresh CVO nanobelt, indicating highly reversible Zn^{2+} intercalation of CVO host without structural breakdown.

Fig. 3d displays the evolution of the (001) peak of CVO electrode in detail during the 3rd CD scan. During the discharge process, Zn^{2+} ions are gradually intercalated into the V_4O_{10} double-layers, leading to a contraction of interlayer spacing, which can be immediately recovered upon voltage reversal. This reversibility and gradual shifting of the (001) peak indicates that the related solid-solution process is associated with Zn^{2+} (de)intercalation from CVO interlayer. We also notice that a peak split appears

when CVO is discharged to 0.8 V, which probably results from a dramatic crystal distortion. At 0.6 V, an obvious peak split is observed. While cycling in a wide voltage window resulted in more Zn^{2+} intercalation, the huge structural stress could lead to very fast capacity decay. Thus, 0.6 V is identified as cut-off voltage for our Zn//CVO cells. About 1.31 Zn/CVO can be intercalated into CVO lattice without apparent crystal breakdown. The *ex-situ* high-resolution TEM analysis provides further proof for the unusual Zn^{2+} storage mechanism of CVO cathodes. As shown in **Fig. 3e**, the ($\bar{\ }$) and (005) planes of pristine CVO nanobelt exhibit lattice fringes with d-spacing of 0.195 and 0.211 nm, respectively. When discharged to 0.6 V, a lattice fringe with d-spacing of 0.188 and 0.19 nm is observed, corresponding to ($\bar{\ }$) and (005) planes, respectively. Such a subtle lattice contraction (3.6-9.9%) is consistent with our XRD data. Impressively, the contracted crystal structure immediately recovered to its initial state (0.195 and 0.201 nm for ($\bar{\ }$) and (005) planes, respectively) upon Zn^{2+} ion removal (1.6 V). These findings match with those deduced from the *ex-situ* XRD and XPS studies: the CVO nanobelt is suitable cathode material for stable aqueous Zn-ion storage. Furthermore, considering the abundance and low cost of both Ca, Zn and V, our Zn//CVO cell presents a potentially safe, durable, and cost-efficient device for large-scale energy storage.

In this communication, calcium vanadium oxide bronze ($Ca_{0.24}V_2O_5$ *0.83*H_2O) nanostructures are synthesized using a one-step hydrothermal method, and used as aqueous ZIB cathodes. The freestanding CVO paper cathode delivers capacities of 340 and 289 mAh g^{-1} at 0.2 and 1 C, respectively. Our Zn//CVO cells show impressive energy density of 267 Wh kg^{-1} at a power density of 53.4 W kg^{-1}, outperforming most of previously reported protypes. Excellent cycling stability (up to 5000 cycles at 80 C) and rate capability were also demonstrated. The structural evolution and electrochemical kinetics were discussed in detail. The low-cost and excellent lifespan show that nanostructured CVO is a viable cathode for aqueous Zn-ion storage.

[1]   aC. Xu, B. Li, H. Du, F. Kang, *Angewandte Chemie International Edition* **2012**, *51*, 933-935; bJ. F. Parker, C. N. Chervin, I. R. Pala, M. Machler, M. F. Burz, J. W. Long, D. R. Rolison, *Science* **2017**, *356*, 415-418; cB. J. Hertzberg, A. Huang, A. Hsieh, M. Chamoun, G. Davies, J. K. Seo, Z. Zhong, M. Croft, C. Erdonmez, Y. S. Meng, *Chem Mater* **2016**, *28*, 4536-4545.

[2]   D. Kundu, B. D. Adams, V. Duffort, S. H. Vajargah, L. F. Nazar, *Nature Energy* **2016**, *1*, 16119.

[3]   aX. Wu, Y. Cao, X. Ai, J. Qian, H. Yang, *Electrochem Commun* **2013**, *31*, 145-148; bC. D. Wessells, S. V. Peddada, R. A. Huggins, Y. Cui, *Nano Lett* **2011**, *11*, 5421-5425; cL. Peng, Y. Zhu, X. Peng, Z. Fang, W. Chu, Y. Wang, Y. Xie, Y. Li, J. J. Cha, G. Yu, *Nano Lett* **2017**, *17*, 6273-6279; dH. Li, L. Peng, Y. Zhu, D. Chen, X. Zhang, G. Yu, *Energ Environ Sci* **2016**, *9*, 3399-3405; eY. Zhu, L. Peng, D. Chen, G. Yu, *Nano Lett* **2015**, *16*, 742-747.

[4]   aX. Wu, Y. Xiang, Q. Peng, X. Wu, Y. Li, F. Tang, R. Song, Z. Liu, Z. He, X. Wu, *J Mater Chem A* **2017**, *5*, 17990-17997; bH. Zhang, K. Ye, S. Shao, X. Wang, K. Cheng, X. Xiao, G. Wang, D. Cao, *Electrochim Acta* **2017**, *229*, 371-379; cS. Liu, J. Hu, N. Yan, G. Pan, G. Li, X. Gao, *Energ Environ Sci* **2012**, *5*, 9743-9746.

[5]   G. Li, Z. Yang, Y. Jiang, C. Jin, W. Huang, X. Ding, Y. Huang, *Nano Energy* **2016**, *25*, 211-217.

[6]   M. Yan, P. He, Y. Chen, S. Wang, Q. Wei, K. Zhao, X. Xu, Q. An, Y. Shuang, Y. Shao, *Adv Mater* **2017**, 1703725.

[7]   aH. Pan, Y. Shao, P. Yan, Y. Cheng, K. S. Han, Z. Nie, C. Wang, J. Yang, X. Li, P. Bhattacharya, *Nature Energy* **2016**, *1*, 16039; bM. H. Alfaruqi, V. Mathew, J. Gim, S. Kim, J. Song, J. P. Baboo, S. H. Choi, J. Kim, *Chem Mater* **2015**, *27*, 3609-3620.

[8]   aL. Zhang, L. Chen, X. Zhou, Z. Liu, *Adv Energy Mater* **2015**, *5*, 1400930; bR. Trócoli, F. La Mantia, *Chemsuschem* **2015**, *8*, 481-485; cZ. Jia, B. Wang, Y. Wang, *Mater Chem Phys* **2015**, *149*, 601-606.

[9]   Y. Ma, H. Zhou, S. Zhang, S. Gu, X. Cao, S. Bao, H. Yao, S. Ji, P. Jin, *Chem-Eur J* **2017** DOI: 10.1002/chem.201702814.

[10]   E. Levi, Y. Gofer, D. Aurbach, *Chem Mater* **2009**, *22*, 860-868.

[11]   Y. Oka, O. Tamada, T. Yao, N. Yamamoto, *J Solid State Chem* **1996**, *126*, 65-73.

[12]   Y. Oka, T. Yao, N. Yamamoto, *J Solid State Chem* **1997**, *132*, 323-329.

[13]   J. Wang, J. Polleux, J. Lim, B. Dunn, *The Journal of Physical Chemistry C* **2007**, *111*, 14925-14931.

[14]   C. Xia, J. Guo, Y. Lei, H. Liang, C. Zhao, H. N. Alshareef, *Adv Mater* **2018**, 30, 1705580.

[15]   P. He, M. Yan, G. Zhang, R. Sun, L. Chen, Q. An, L. Mai, *Adv Energy Mater* **2017**, *7*, 1601920.

[16]   Z. Liu, P. Bertram, F. Endres, *J Solid State Electr* **2017**, 1-7.

[17]   B. Zhang, Y. Liu, X. Wu, Y. Yang, Z. Chang, Z. Wen, Y. Wu, *Chem Commun* **2014**, *50*, 1209-1211.

[18]   S. Jeong, J. Boo, *Thin Solid Films* **2004**, *447*, 105-110.

[19]   ŒĒŌ å &˝æ Sánchez, E. Alvarez-Ayuso, *Miner Eng* **2002**, *15*, 539-547.

COMMUNICATION

Layered calcium vanadium oxide bronze was synthesized for aqueous zinc-ion battery applications. We demonstrate that the calcium based bronze shows promising performance for Zn^{2+} storage in aqueous electrolyte. The Zn cell delivers an energy density of 267 Wh kg^{-1} at a power density of 53.4 W kg^{-1}.
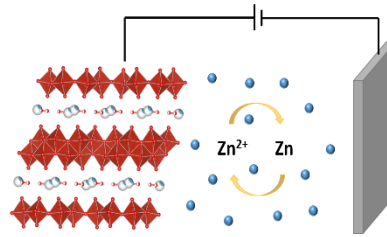
Chuan Xia, Jing Guo, Peng Li, Xixiang Zhang and Husam Alshareef*

Page No. – Page No.

Highly Stable Aqueous Zinc-ion Storage Using Layered Calcium Vanadium Oxide Bronze Cathode